Advanced Energy Conversion Materials
http://ojs.wiserpub.com/index.php/AECM/

UNIVERSAL WISER PUBLISHER

Review

Optical, Surface and Photocatalytic Properties of Rare Earth Elements (Er-Gd) Doped CeO_2 Films

Seniye Karakaya*, Leyla Kaba

Department of Physics, Eskisehir Osmangazi University, TR-26040 Eskisehir, Turkey
E-mail: seniyek@ogu.edu.tr

Received: 22 March 2024; **Revised:** 26 April 2024; **Accepted:** 26 April 2024

Abstract: Er/Gd co-doped CeO_2 thin films were produced by the ultrasonic spray pyrolysis technique (USP) and photocatalytic degradation of methylene blue (MB) dye was carried out. The effect of Er/Gd co-doping on the optical, surface and photocatalytic properties of CeO_2 films was analyzed. All prepared films showed high transmittance of over 75% in the visible region (300-900 nm). According to FESEM analysis results, morphological changes such as cracks and particle agglomeration were observed in the films. In photoluminescence measurements, blue and green emissions were found in the films. While the photocatalytic degradation percentage of the undoped CeO_2 film was 42%, when both Er and Gd were doped, the degradation percentage increased significantly and reached 75%. Photocatalytic studies revealed that Er/Gd-doped CeO_2 films exhibited better photocatalytic efficiency compared to undoped CeO_2 films. As a result, it was observed that the coexistence of Er and Gd has significant effects on the optical, surface and photocatalytic properties of CeO_2 films. Considering all the results, it is concluded that CeO_2:Er:Gd photocatalysts may have an important potential application in environmental remediation.

***Keywords*:** Er/Gd co-doped CeO_2 films, methylene blue, photocatalytics, environmental remediation

1. Introduction

Untreated industrial wastewater is one of the main sources of pollution. Pollution of water resources constitutes one of the most important problems of the modern world. The need for efficient and stable materials that can be used as photocatalysts under visible light in wastewater treatment has increased in recent years. Especially metal oxide semiconductors have been attracting much interest [1]. ZnO [2], Fe_2O_3 [3], SnO_2 [4], WO_3 [5], TiO_2 [6] and CeO_2 [7] are used for the removal of organic contaminants from various pollution sources because of their high photo-activity. Among these materials, except TiO_2, CeO_2 is one of the materials most frequently applied as a semiconductor [8]. CeO_2 is an n-type semiconductor metal oxide, it has several properties such as chemical inactivity, cost-effectiveness, photostability and non-toxicity [9]. CeO_2 is a relatively stable rare earth oxide that has good properties for the storage and release of oxygen. When the valencies change, oxygen vacancies or lattice defects form due to the loss of oxygen or electrons. The crystal is a cubic fluorite structure [10]. Furthermore, CeO_2 films can be very useful as an energy storage material [11], gas sensors [12], photocatalysis [13], solid solutions [14], optoelectronics [15], catalysts [16], supercapacitors [17], UV photodetectors [18]. Optical and surface properties are among the important parameters [19-21]. As a rare earth element, the 'Er' constituent has gained important interest as a dopant due to its promising physical and

DOI: https://doi.org/10.37256/aecm.5120244634

chemical characteristics [22]. Among the various rare earth oxide materials studied so far, CeO_2 is the best base material for other rare earth materials such as europium (Eu), yttrium (Yt), gadolinium (Gd), samarium (Sm) and erbium (Er). CeO_2 NPs attract attention due to their properties such as UV absorbing capacity [23]. Er and Gd elements were doped separately into CeO_2 films and studied [24-27]. Only one study on Er and Gd co-doped CeO_2 films has been found in the literature. This work, published in the literature by Torun and his group [28], is to synthesize Er and Er-Gd co-dopants as electrolyte additives, so an investigation on their photocatalytic properties has not been studied. So far, there is no study in the literature focusing on the photocatalytic properties of CeO_2 films doped with Er and Gd elements. The aim of this study is to investigate the optical, surface and photocatalytic properties of Er and Er/Gd co-dopants on CeO_2 films in order to fill this gap in the literature.

2. Experimental

2.1 *Material and methods*

Undoped CeO_2, CeO_2:Er (3%) and CeO_2:Er:Gd (3%) co-doped thin films were obtained using the ultrasonic spray pyrolysis technique (USP). Before deposition, the glass substrates were cleaned with detergent, then rinsed with deionized water and acetone, followed by a final rinse with deionized water. The precursor solution of cerium nitrate hexahydrate $Ce(NO_3)_3 \cdot 6H_2O$ was dissolved in 75 ml methanol and 25 ml deionized water (3:1) and stirred on a magnetic stirrer at 60 °C for 15 min. Solutions of erbium nitrate pentahydrate $Er(NO_3)_3 \cdot 5H_2O$ and gadolinium nitrate hexahydrate $Gd(NO_3)_3 \cdot 6H_2O$ were also prepared and added to the precursor solution. Experimental parameters such as substrate temperature, solution flow rate and time required for the synthesis are given in Table 1. During the synthesis process, the substrate temperature and solution flow rate parameters were continuously controlled. The controlled parameters have significant effects on the resulting films. Low or high base temperature significantly affects the adhesion of the films to the substrate and their physical properties. Increasing and decreasing the solution flow rate causes porous films to form or not.

Table 1. Experimental parameters for deposition of undoped CeO_2, CeO_2:Er (3%) and CeO_2:Er:Gd (3%) thin films

Film	CeO_2, CeO_2:Er and CeO_2:Er:Gd
Solvent	Methanol:Deionized water (3:1)
Solution Molarity and Amount	0.05 M, 100 ml
Doping Concentration (%)	3
Substrate Temperature	300 ± 5 °C
Solution Flow Rate and Time	10 ml/min, 10 min

2.2 *Physical measurements*

Transmittance for visible light was determined by using the Perkin Elmer Schimadzu UV-2550 spectrophotometer. Structural properties of the films were performed using XRD patterns ‘‘Panalytical Empyrian’’ with CuKα radiation. AFM and FESEM devices have been used to obtain the information of the surface properties. Photoluminescence (PL) spectra of the films have been taken at 350 nm excitation wavelength using the Perkin Elmer LS55 Fluorescence Spectrometer system. The maximum absorption wavelengths of the dye solutions used in photocatalytic activity measurement were determined using a UV-2550 spectrophotometer. Photodegradation efficiency (%) was determined by

measuring the absorbance of the samples using Perkin Elmer Schimadzu UV-2550 spectrophotometer.

3. Results and discussion

3.1 *Optical properties*

The transmittance and absorbance spectra of CeO_2, CeO_2:Er and CeO_2:Er:Gd thin films are shown in Figure 1. All films show high transparency between 75% and 90% in the 300-900 nm visible range. The CeO_2:Er (3%) film has the highest transmittance of over 90% in the visible range.

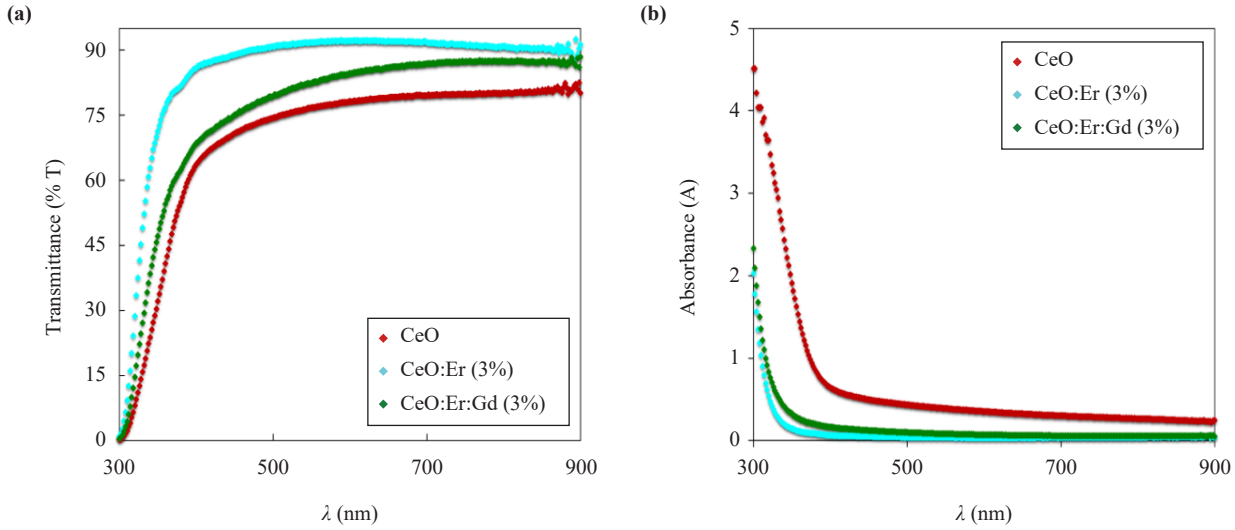

Figure 1. (a) The transmittance and (b) absorbance spectra of undoped CeO_2, CeO_2:Er (3%) and CeO_2:Er:Gd (3%) films

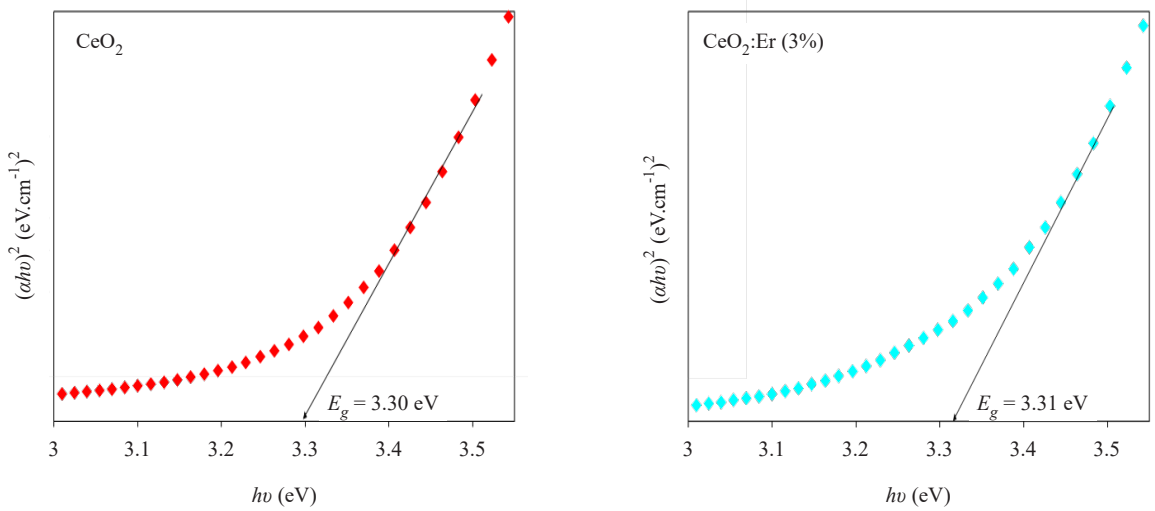

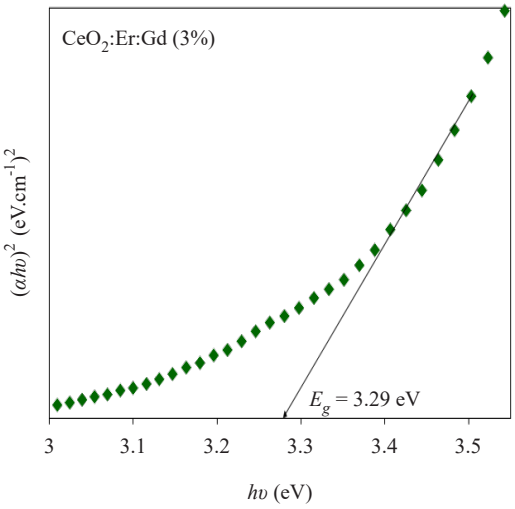

Figure 2. Optical band gap of undoped CeO_2, CeO_2:Er (3%) and CeO_2:Er:Gd (3%) films

The Tauc relationship was used to directly determine the optical band gap energy of the produced thin films. Figure 2 shows the change of $(\alpha h\upsilon)^2$ with energy $h\upsilon$ for a direct transition using the Tauc formula [29];

$$(\alpha h\upsilon)^2 = A\left(h\upsilon - E_g\right) \tag{1}$$

where α absorption coefficient, $h\upsilon$ incident photon energy, A proportionality constant and E_g optical band gap. Figure 2 shows the optical bandgap values graph.

3.2 *Structural properties*

Figure 3 represents the XRD pattern of pure CeO_2, CeO_2:Er (3%) and CeO_2:Er:Gd (3%) films and the observed peaks correspond to (111), (200), (220) and (311). All characteristic peaks matched JCPDS card no. 34-0394 [30]. The (111) peak orientation was dominant in the undoped CeO_2, CeO_2:Er (3%) and CeO_2:Er:Gd (3%) co-doped films. The high intensity diffraction peak (111) shifts slightly towards the lower angle as a result of the incorporation of Gd^{3+} ions. This shift in the peak may be related to the lattice expansion and strain induced by the doping of Gd ions [26].

Crystallite size (D) is estimated using the Scherrer formula [31]:

$$D = \frac{k\lambda}{\beta \cos\theta} \tag{2}$$

where (D) is the crystallite size in nanometer scale, k (0.9) is the Scherrer constant, λ is the X-ray wavelength (0.15406 nm), β is full width at the half of maximum peak (FWHM) and θ is the Bragg's angle.

Dislocation density (δ) is obtained by the following formula [32]:

$$\delta = \frac{1}{D^2} \tag{3}$$

Table 2. Crystallite size (D) and dislocation density (δ) values for the (111) plane of undoped CeO_2, CeO_2:Er (3%) and CeO_2:Er:Gd (3%) films

Film	D (nm)	$\delta \times 10^{-4}$ (1/nm^2)
CeO_2	21.83	21
CeO_2:Er (3%)	16.05	39
CeO_2:Er:Gd (3%)	13.15	58

Table 2 shows that the average crystallite size decreased from 21.83 nm to 13.15 nm with the addition of Er and Er/Gd.

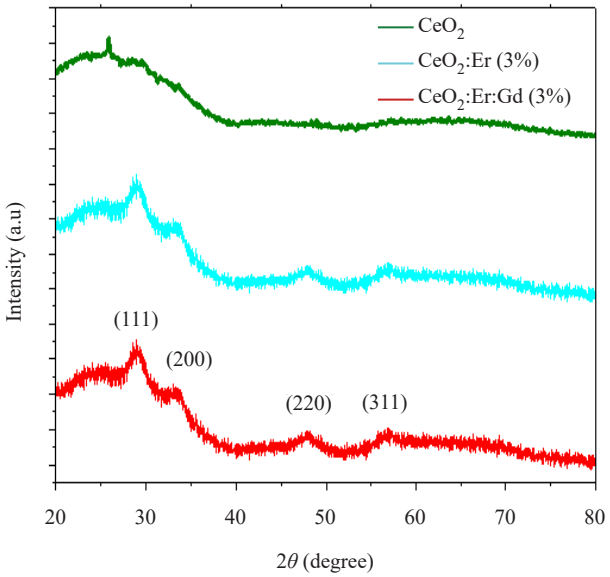

Figure 3. XRD patterns of undoped CeO_2, CeO_2:Er (3%) and CeO_2:Er:Gd (3%) films

3.3 *Afm analysis*

The surface properties of the films were examined using AFM. Figure 4 shows the 3D surface images of CeO_2 thin films taken from an area of 10 ×10 μm. The morphology of undoped CeO_2 and Er-doped CeO_2 thin films exhibits spherical small granules with homogeneous distribution. It can be seen from AFM images that the film morphology changes with Er/Gd doping. Additionally, Table 3 gives the R_q (root mean square) and R_a (average) roughness values of the films. The roughness values given in Table 3 refer to the scanned areas. The sample with the highest surface roughness among all films is CeO_2:Er:Gd (3%). The roughness values of films to be used in technological and photocatalytic applications are significant [33].

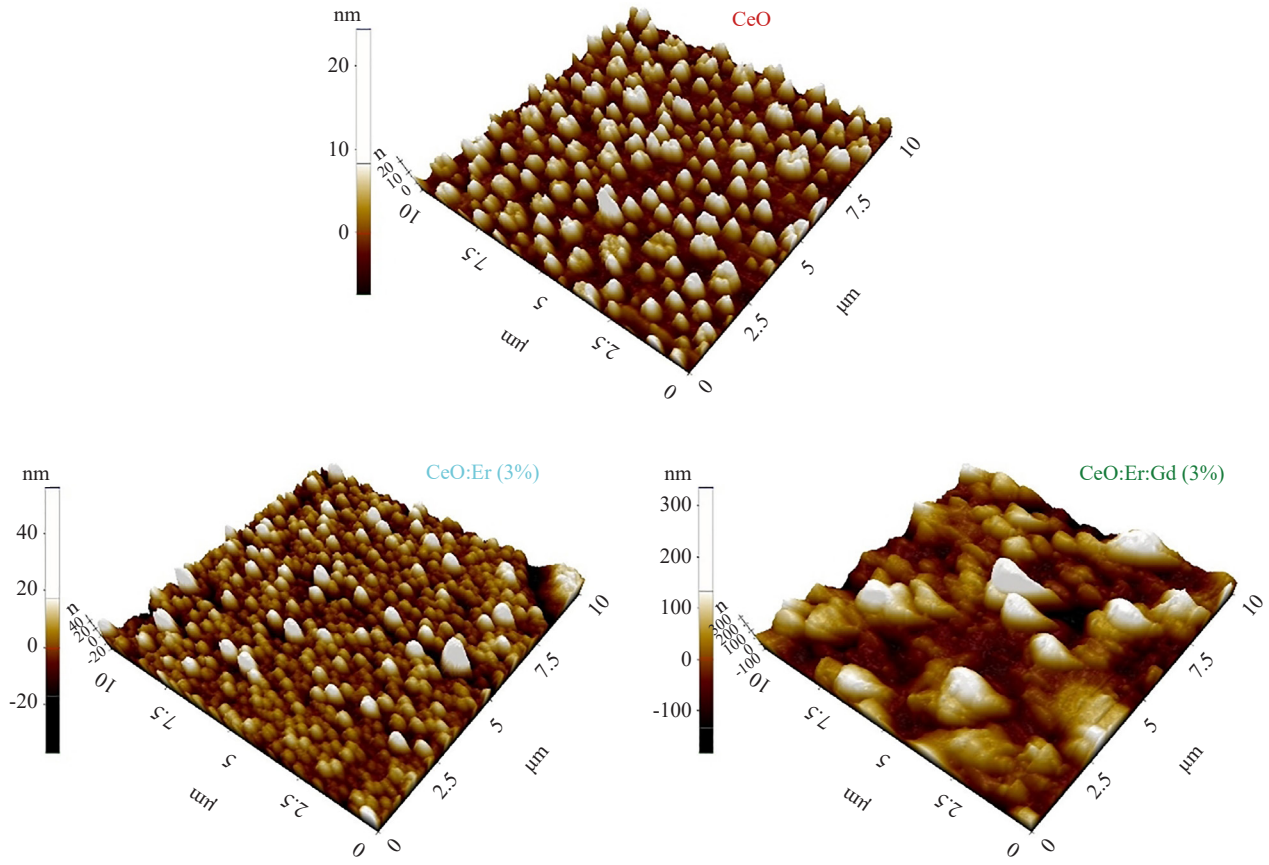

Figure 4. AFM images of undoped CeO_2, CeO_2:Er (3%) and CeO_2:Er:Gd (3%) films

Table 3. R_q and R_a values of undoped CeO_2, CeO_2:Er (3%) and CeO_2:Er:Gd (3%) films

Film	R_q (*nm*)	R_a (*nm*)
CeO_2	4.2	3.5
CeO_2:Er (3%)	47.3	36.6
CeO_2:Er:Gd (3%)	68.1	52.9

3.4 *Morphology analysis*

The surface morphology of the films was investigated using FESEM. Figure 5 shows FESEM and EDX micrographs of CeO_2, CeO_2:Er and CeO_2:Er:Gd films at 2 μm and 500 nm magnification. A cracked surface is seen in the FESEM images (Figure 5) of undoped CeO_2 and CeO_2:Er doped films. After Er/Gd co-doping of CeO_2 films, agglomeration of particles was observed via FESEM analysis images. Grained structures overlap to form agglomerates and cracks may represent boundaries between agglomerates [34]. It was observed that the surface morphology of the films changed with co-doping. The quality of the surface is important for applications such as sensing and photocatalysis [35]. Improvement of photocatalytic activity depends on various factors. Among these factors, surface morphology and surface roughness are important factors. In Figure 4, the density and surface area of particle agglomeration increases

with Er-Gd co-doping. Particle agglomeration creates rough surfaces. Surface roughness values are listed in Table 3. The EDX study helps us identify the elemental compositions of the deposited films and is reported in Table 4. As seen in Table 4, Ce, O, Er and Gd element ratios were determined by EDX.

Table 4. EDX results for undoped CeO_2, CeO_2:Er (3%) and CeO_2:Er:Gd (3%) films

Film	Ce wt%	O wt%	Er wt%	Gd wt%
CeO_2	69.15	30.85	-	-
CeO_2:Er (3%)	19.42	76.49	4.09	-
CeO_2:Er:Gd (3%)	37.63	54.36	7.58	0.42

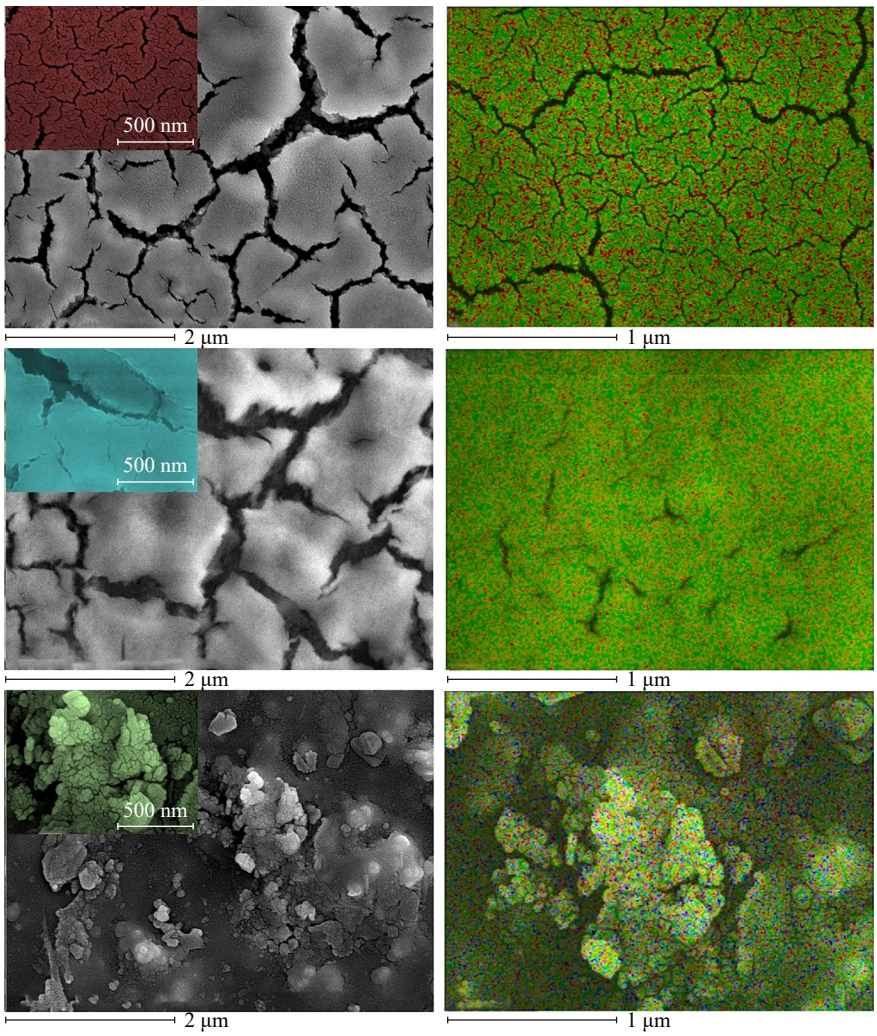

Figure 5. FESEM surface of undoped CeO_2, CeO_2:Er (3%) and CeO_2:Er:Gd (3%) films taken at (a) 2 µm and 500 nm magnification, (b) Undoped CeO_2, CeO_2:Er (3%) and CeO_2:Er:Gd (3%) films elemental mapping images.

3.5 *Photoluminescence properties*

PL spectra can be used to determine the bandgap of the material and to investigate the traps caused by visible deep defects in the material [36]. Emission spectra of undoped CeO_2, CeO_2:Er and CeO_2:Er:Gd films were obtained at 350 nm excitation wavelength at room temperature (Figure 6). Labelled A and B are emission peaks representing two different luminescence transitions. Blue and green emissions were observed in all films. The presence of the blue emission is thought to be related to the level of imperfection due to dislocation and oxygen defects that are localized between the O 2p and Ce 4f bands [37]. It suggests that increasing the Gd doping concentration may increase surface defect levels and suppress electron transfer from Ce 4f to O 2p levels [38]. Green emission at ~565 nm in CeO_2 film can be caused by surface defects, and the high intensity of green emission can be attributed to the high density of oxygen vacancies [39]. The green emission peaks at ~565 nm correspond to the transition from the conduction band to the Gd^{3+} dopant level and the recombination of electrons trapped in the singly ionized oxygen vacancy (V_{o+}) with holes in the valence band, respectively [40]. Since PL emission spectra are generated by the recombination of excited electrons and holes, an increase in PL intensity would indicate an increase in the recombination fraction of electron-hole pairs under the influence of light irradiation [37].

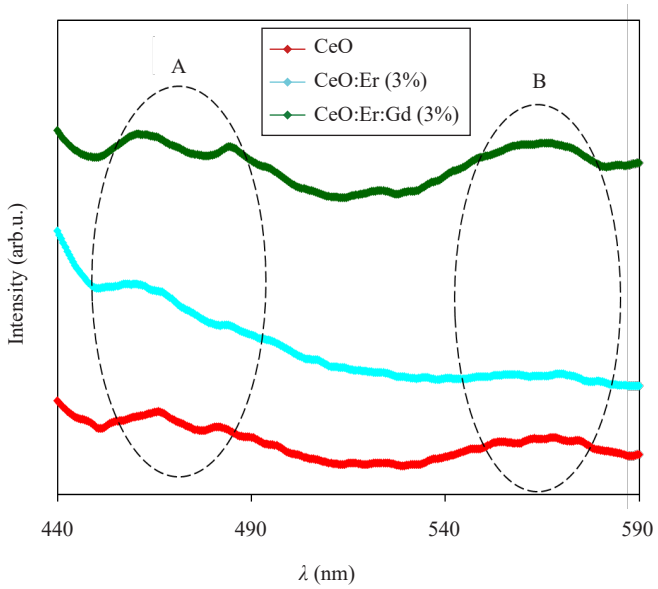

Figure 6. PL spectra of undoped CeO_2, CeO_2:Er (3%) and CeO_2:Er:Gd (3%) films

3.6 *Photocatalytic activity*

The photocatalytic performance of the produced thin films was evaluated by examining the decolorization of high-purity MB organic dye solution with an initial concentration (C_0) of 2 mg/L. In the presence of undoped CeO_2, CeO_2:Er (3%) and CeO_2:Er:Gd (3%) co-doped thin films, the photodegradation of MB dye proceeds quite well during 300 min of irradiation. Under 300 minutes of illumination, degradation efficiency increased with doping. The percent degradation efficiency of CeO_2 films is given in Figure 7.

The photocatalytic degradation efficiency was calculated by the following equation [41];

$$\eta(\%) = \left(1 - C_t / C_0\right) \times 100 \tag{4}$$

where C_0 represents the initial concentration of MB and C_t denotes the real-time concentrations of MB, respectively.

Surface roughness is one of the important parameters that improve photocatalytic activity. The improvement in photocatalytic degradation percentages with the doping process of the films is supported by the increase in the roughness values presented in Table 3. Another important parameter affecting the photocatalytic activity is the surface defects that occur in photoluminescence measurements. The higher the photoluminescence intensity of the films, the higher the surface defects that occur. The increase in photocatalytic activity as a result of the co-doping process may be due to the fact that the two doped elements are rare earth elements and surface defects formed as a result of doping. Several RE metal ion-modified photocatalysts show higher absorption in the UV region and the higher activity may also be due to its higher intrinsic absorptivity. The higher activity under UV irradiation is probably due to the ability of RE metal ions to trap electrons and minimize electron-hole recombination [42]. These defects are caused by the lifetime of photoexcited holes and electrons and increase the photocatalytic activity by creating electron-hole pair separation [43].

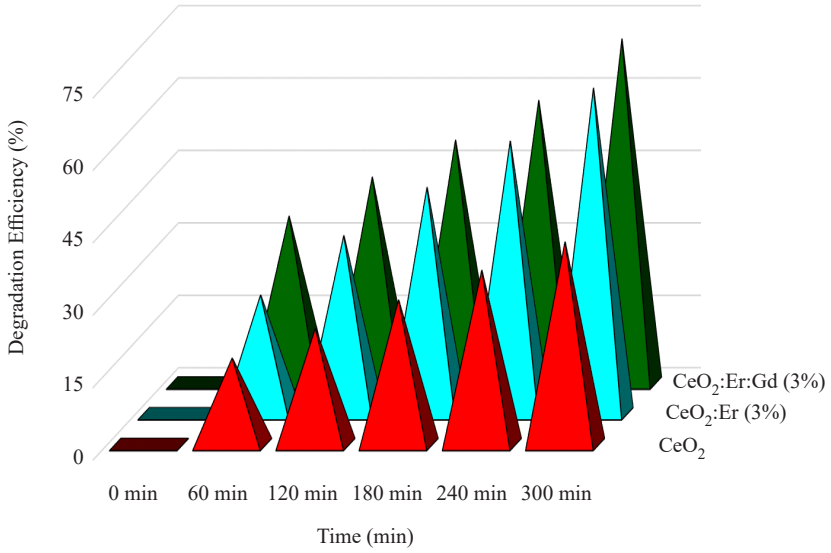

Figure 7. Graph of the degradation efficiency of undoped CeO_2, CeO_2:Er (3%) and CeO_2:Er:Gd (3%) thin films

4. Conclusions

As a result, CeO_2, CeO_2:Er and CeO_2:Er:Gd thin films were deposited on the glass substrate by ultrasonic spray pyrolysis method. Optical, morphological, photoluminescence and photocatalytic properties were evaluated. The optical transmittance of the films was increased by the doping process. Among all films, CeO_2:Er (3%) film stands out with 90% high transmittance. In the AFM analysis results, the film with the highest roughness was seen as CeO_2:Er:Gd (3%). In the FESEM analysis, cracked and particle-agglomerated surfaces were observed in the morphology of the films. Looking at the photoluminescence measurement results, blue and green emission is seen in all films. When the photocatalytic activities of the films were examined, Er/Gd-doped CeO_2 showed a degradation of ~75%, while undoped CeO_2 also showed a degradation of ~42%. Therefore, the best photocatalytic activity was obtained with Er/Gd doped CeO_2. Co-doping of Er/Gd elements has a positive effect on the photocatalytic properties of CeO_2 films. The results show that Er/Gd co-doped CeO_2 nanostructured films are promising for photocatalysts.

Author contributions

Seniye Karakaya: Contributed to conceptualization, writing-review and editing, supervision.

Leyla Kaba: Writing & Editing.

Conflict of interest

The authors declare no competing financial interest.

References

[1] Kusmierek EA. A CeO_2 semiconductor as a photocatalytic and photoelectrocatalytic material for the remediation of pollutants in industrial wastewater: A review. *Catalysts*. 2020; 10(12): 1435.

[2] Karakaya S, Kaba L. Effect of fluorine doping on the improvement of electrical and photocatalytic properties of ZnO films. *Applied Physics A.* 2024; 130(3): 167.

[3] Mami A, Saafi I, Larbi T, Messaoud KB, Yacoubi N, Amlouk M. Unraveling the effect of thickness on the structural, morphological, opto-thermal and DFT calculation of hematite Fe_2O_3 thin films for photo-catalytic application. *Journal of Materials Science: Materials in Electronics*. 2021; 32: 17974-17989.

[4] Bezzerrouk MA, Bousmaha M, Hassan M, Akriche A, Kharroubi B, Naceur R, et al. Enhanced methylene blue removal efficiency of SnO_2 thin film using sono-photocatalytic processes. *Optical Materials*. 2021; 117: 111116.

[5] Abbaspoor M, Aliannezhadi M, Tahrani FS. High-performance photocatalytic WO_3 nanoparticles for treatment of acidic wastewater. *Journal of Sol-Gel Science and Technology*. 2023; 105: 565-576.

[6] Dong X, Mamat M, Baikeli Y, Liu G, Xiaerding F. Effect of Fe doping on crystalline phase, structure and photocatalytic properties of TiO_2 thin films. *Optical Materials*. 2024; 150: 115196.

[7] Choudhary S, Sahu K, Bisht A, Singhal R, Mohapatra S. Template-free and surfactant-free synthesis of CeO_2 nanodiscs with enhanced photocatalytic activity. *Applied Surface Science*. 2020; 503: 144102.

[8] Murugadoss G, Kumar MR, Murugan D, Koutavarapu R, Al-Ansari MM, Aldawsari M. Ultra-fast photocatalytic degradation and seed germination of band gap tunable nickel doping ceria nanoparticles. *Chemosphere.* 2023; 333: 138934.

[9] Murugadoss G, Kumar DD, Kumar MR, Venkatesh N, Sakthivel P. Silver decorated CeO_2 nanoparticles for rapid photocatalytic degradation of textile rose bengal dye. *Scientific Reports*. 2021; 11: 1080.

[10] Cui Z, Zhang L, Xue Y, Feng Y, Wang M, Chen J, et al. Effects of shape and particle size on the photocatalytic kinetics and mechanism of nano-CeO_2. *International Journal of Minerals, Metallurgy and Materials*. 2022; 29: 2221. Available from: https://doi.org/10.1007/s12613-021-2332-0.

[11] Khan AJ, Hanif M, Javed MS, Hussain S, Zhong W, Saleem M, et al. Energy storage properties of hydrothermally processed, nanostructured, porous CeO_2 nanoparticles. *Journal of Electroanalytical Chemistry*. 2020; 865: 114158.

[12] Li P, Wang B, Qin C, Han C, Sun L, Wang Y. Band-gap-tunable CeO_2 nanoparticles for room-temperature NH_3 gas sensors. *Ceramics International.* 2020; 46: 19232-19240.

[13] Mittal M, Gupta A, Pandey OP. Role of oxygen vacancies in Ag/Au doped CeO_2 nanoparticles for fast photocatalysis. *Solar Energy.* 2018; 165: 206-216.

[14] Fang P, Luo MF, Lu JQ, Cen SQ, Yan XY, Wang XX. Studies on the oxidation properties of nanopowder CeO_2-based solid solution catalysts for model soot combustion. *Thermochimica Acta.* 2008; 478: 45-50.

[15] Jayakumar G, Irudayaraj AA, Raj AD, Sundaram SJ, Kaviyarasu K. Electrical and magnetic properties of nanostructured Ni doped CeO_2 for optoelectronic applications. *Journal of Physics and Chemistry of Solids.* 2022; 160: 110369.

[16] Salaev MA, Salaeva AA, Kharlamova TS, Mamontov GV. Pt-CeO_2-based composites in environmental catalysis: A review. *Applied Catalysis B: Environmental.* 2021; 295: 120286.

[17] Das HT, Balaji TE, Dutta S, Das N, Das P, Mondal A, et al. Recent trend of CeO_2-based nanocomposites electrode in supercapacitor: A review on energy storage applications. *Journal of Energy Storage.* 2022; 50: 104643.

[18] Zinzuvadiya S, Pandya NC, Joshi US. Optoelectronic response of (111) oriented CeO_2 films for UV photodetector. *Thin Solid Films.* 2019; 669: 525-530.

[19] Ijaz U, Siyar M, Park C. The power of pores: Review on porous thermoelectric materials. *RSC Sustainability.* 2024; 2: 852-870.

[20] Khan H, Siyar M, Park C, Javaid F, Umer MA, Jin W, et al. Tuning the electronic properties in facile in-situ solution synthesis of $SnSe_2$/rGO nanocomposites with enhanced thermoelectric performance. *Journal of Materials*

Research. 2023; 38: 16.
[21] Siyar M, Maqsood A, Khan SB. Synthesis of mono layer graphene oxide from sonicated graphite flakes and their hall effect measurements. *Materials Science-Poland.* 2014; 32(2): 292-296.
[22] Poornaprakash B, Chalapathi U, Kumar M, Subramanyam K, Vattikuti SVP, Reddy MSP, et al. Enhanced photocatalytic activity and hydrogen evolution of CdS nanoparticles through Er doping. *Ceramics International.* 2020; 46: 21728-21735.
[23] Kundu S, Sutradhar N, Thangamuthu R, Subramanian B, Panda AB, Jayachandran M. Fabrication of catalytically active nanocrystalline samarium (Sm)-doped cerium oxide (CeO_2) thin films using electron beam evaporation. *Journal of Nanoparticle Research*. 2012; 14: 1040. Available from: https://doi.org/10.1007/s11051-012-1040-0.
[24] Chahal S, Kumar A, Kumar P. Erbium-doped oxygen deficient cerium oxide: Bi-functional material in the field of spintronics and photocatalysis. *Applied Nanoscience.* 2020; 10: 1721-1733.
[25] Magdalane CM, Kaviyarasu K, Raja A, Arularasu MV, Mola GT, Isaev AB, et al. Photocatalytic decomposition effect of erbium doped cerium oxide nanostructures driven by visible light irradiation: Investigation of cytotoxicity, antibacterial growth inhibition using catalyst. *Journal of Photochemistry & Photobiology, B: Biology.* 2018; 185: 275-282.
[26] Abushad M, Khan W, Arshad M, Husain S, Ansari A, Chakradhary VK. Compositional disorder and its effect on optical and photocatalytic properties of $Ce_{1-x}Gd_xO_2$ ($0 \leq x \leq 0.20$) nanostructures. *Journal of Materials Science: Materials in Electronics*. 2023; 34: 710.
[27] Madaan V, Kumar K. Remediation of industrial pollutants in wastewater by photocatalytic treatment with Gadolinium doped CeO_2 with composition $Gd_xCe_{1-x}O_2$ ($0 < x < 0.1$). *Journal of Physics and Chemistry of Solids.* 2023; 178: 111344.
[28] Ozlu TH, Çakar S. Thermal characterization of Er-doped and Er-Gd co-doped ceria-based electrolyte materials for SOFC. *Journal of Thermal Analysis and Calorimetry*. 2018; 133: 1233-1239.
[29] Tauc J, Grigorovici R, Vancu A. Optical properties and electronic structure of amorphous germanium. *Physica Status Solidi B: Basic Solid State Physics.* 1966; 15(2): 627-637.
[30] Soni B, Makkar S, Biswas S. Effects of surface structure and defect behavior on the magnetic, electrical, and photocatalytic properties of Gd-doped CeO_2 nanoparticles synthesized by a simple chemical process. *Materials Characterization.* 2021; 174: 110990.
[31] Dumrongrojthanath P, Phuruangrat A, Sakhon T, Thongtem T, Thongtem S. Effect of Gd dopant on visible-light-driven photocatalytic properties of CeO_2 nanowires synthesized microwave-assisted hydrothermal method. *Russian Journal of Inorganic Chemistry.* 2022; 67(11): 1880-1887.
[32] Prakash RS, Chandrasekaran J, Vivek P, Balasubramani V. Improvement of optoelectronic properties of in doped CeO_2 thin films for photodiode applications. *Inorganic Chemistry Communications.* 2023; 151: 110592.
[33] Sani ZK, Ghodsi FE, Mazloom J. Photoluminescence and electrochemical properties of transparent CeO_2-ZnO nanocomposite thin films prepared by Pechini method. *Applied Physics A: Materials Science & Processing.* 2017; 123: 121.
[34] El-Habib A, Brioual B, Bouachri M, Zimou J, Aouni A, Diani M, et al. Synthesis and characterization of Nd-doped CeO_2 thin films grown by spray pyrolysis method: Structural, optical and electrochemical properties. *Surfaces and Interfaces.* 2024; 45: 103859.
[35] Acosta-Silva YJ, Castañedo-Perez R, Torres-Delgado G, Méndez-López A, Zelaya-Ángel O. Effect of annealing temperature on structural, morphological and optical properties of CeO_2 thin films obtained from a simple precursor solution. *Journal of Sol-Gel Science and Technology.* 2017; 82: 20-27.
[36] Kurtaran S, Kellegöz M, Köse S. Characterization of Gd doped CeO_2 thin films grown by ultrasonic spray pyrolysis. *Optical Materials.* 2021; 117: 111144.
[37] El Desouky FG, Saadeldin MM, Mahdy MA, Abd El Wahab SM, El Zawawi IK. Impact of calcination temperature on the structure, optical and photoluminescence properties of nanocrystalline cerium oxide thin films. *Materials Science in Semiconductor Processing.* 2020; 111: 104991.
[38] Khadar YAS, Balamurugan A, Devarajan VP, Subramanian R. Hydrothermal synthesis of Gadolinium (Gd) doped cerium oxide (CeO_2) nanoparticles: Characterization and antibacterial activity. *Oriental Journal of Chemistry.* 2017; 33(5): 2405-2411.
[39] Rzaij JM. A novel room-temperature nitrogen dioxide gas sensor based on silver-doped cerium oxide thin film. *Sensors & Actuators: A. Physical.* 2023; 363: 114748.
[40] Sakthivel P, Asaithambi S, Karuppaiah M, Yuvakkumar R, Hayakawa Y, Ravi G. Improved optoelectronic properties of Gd doped cadmium oxide thin films through optimized film thickness for alternative TCO applications. *Journal of Alloys and Compounds.* 2020; 820: 153188.

[41] Cuadra JG, Estrada AC, Oliveira C, Abderrahim LA, Porcar S, Fraga D, et al. Functional properties of transparent ZnO thin films synthetized by using spray pyrolysis for environmental and biomedical applications. *Ceramics International.* 2023; 49: 32779-32788.
[42] Weber AS, Grady AM, Koodali RT. Lanthanide modified semiconductor photocatalysts. *Catalysis Science & Technology.* 2012; 2: 683-693.
[43] Karakaya S, Kaba L. Wrinkle type nanostructured of Al-Ce co-doped ZnO thin films for photocatalytic applications. *Surfaces and Interfaces.* 2024; 44: 103655.